Advanced Development of Space Photovoltaic Concentrators Using Robust Lenses, Multi-Junction Cells, & Graphene Radiators

Mark O'Neill[1], A.J. McDanal[1], Michael Piszczor[2], Timothy Peshek[2], Matthew Myers[2], Claiborne McPheeters[3], Jeff Steinfeldt[3], Benjamin Heintz[3], Paul Sharps[3], Megan Puglia[4], Challa Kumar[4]

[1]Mark O'Neill, LLC, Keller, TX 76248, [2]NASA Glenn Research Center, Cleveland, OH 44135, [3]SolAero Technologies, Albuquerque, NM 87123, [4]University of Connecticut, Storrs, CT 06269

***Abstract* — At the past three PVSCs [1]-[3], our team has presented recent advances in our space photovoltaic concentrator technology. In the past year, under multiple NASA-funded research and technology development programs, our team has made much additional progress in the advanced development of space photovoltaic concentrators. New robust Fresnel lenses, new high-efficiency multi-junction cells, and new graphene radiators have been developed. The paper will present the latest advances in this technology.**

***Index Terms* — concentrator, Fresnel lens, multi-junction cells, ultralight, graphene.**

I. Introduction and Summary

As discussed in our team's papers at the last three PVSCs [1]-[3], we have been working for the past several years on advanced space photovoltaic concentrator technology using three key elements:

1. Ultralight, robust, color-mixing, flat Fresnel lens optical elements. The latest lenses are strengthened with either:
    1. A ceria-doped glass superstrate to support the silicone prisms forming the lens, or
    2. embedded mesh in the silicone lens itself.
2. Advanced multi-junction solar cells of two types:
    1. 3-junction germanium based solar cells, and
    2. inverted metamorphic multi-junction (IMM) solar cells with at least 4 junctions to enhance conversion efficiency.
3. Waste heat radiators made from graphene, a new material with unprecedented in-plane thermal conductivity. The latest radiators also have new features:
    1. The graphene is deposited onto the back side of a reflective aluminum foil top surface using innovative methods, and
    2. The bi-material radiator can mitigate both low-intensity, low-temperature (LILT) effects and high-intensity, high-temperature (HIHT) effects for near-sun and deep space missions, respectively.

While we have developed both 4X line-focus concentrators requiring only single-axis sun-tracking and 25X point-focus concentrators requiring two-axis sun-tracking, the latter has been under more intense development for the past year primarily because of its superior ability to mitigate low-intensity, low-temperature (LILT) problems for deep space missions. In the paragraphs below, we will therefore present technology advances in the past year for this point-focus concentrator technology.

II. Description of the Concentrator Module

Fig. 1 shows the point-focus concentrator module, including the lens, the photovoltaic cell assembly, and the graphene-based radiator. Fig. 1 also summarizes the methods of mitigating LILT and HIHT cell problems for the new concentrator. Even deep space missions often use a near-sun inner planet fly-by as a gravity assist maneuver to reduce the propellant needed to reach an outer planet, exposing the cells to both HIHT and LILT effects over the mission. A simple reduction in lens-to-cell spacing can be used to defocus the lens so that a desired fraction of the focused sunlight misses the cell and reflects away from the radiator. For a Venus swing-by, since Venus is about 0.7 astronomical units (AU) from the sun compared to Earth at 1.0 AU, the solar irradiance is about twice as high near Venus compared to near Earth. Reflecting half the focused sunlight away will therefore keep the cell temperature and the power output at approximately the same value as at 1 AU with the cell

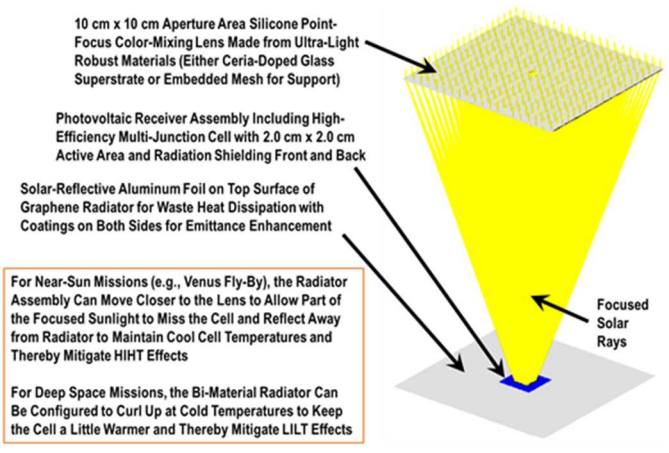

Fig. 1. 25X Point-Focus Space Photovoltaic Concentrator.

in its normal position relative to the lens. This concentrator technology will be deployed and supported as a dual (lens blanket and radiator blanket) flexible-blanket array, and the HIHT mitigation will be accomplished by moving the two blankets slightly closer together at array to sun distances less than 1 AU.

LILT mitigation for deep space missions is two-fold. The low-intensity (LI) problem is mitigated by the 25X concentration. For a Jupiter mission, since Jupiter is at about 5 AU, the solar irradiance is about $1/25^{th}$ as high as near Earth. A one-sun array would thus have only $1/25^{th}$ as much cell current near Jupiter compared to near Earth. But the 25X lens increases the cell irradiance to about the same value as a one-sun cell near earth. The low-temperature (LT) problem can be mitigated by allowing the bi-material radiator to curl up due to differential thermal contraction, reducing the radiator view factor to deep space. With the radiator and cell temperatures a little above the glass transition temperature of the silicone used in both, stresses can be reduced. This "nyctinastic radiator" technology is being developed under a NASA STTR program.

III. Recent Lens Developments

In the past year, we have developed two new styles of robust point-focus lenses:

1. A thicker ceria-doped glass superstrate lens using 100-micron CMG glass from Qioptiq to support the 100-micron-tall silicone prisms on the inside surface of the lens, and
2. New embedded meshes to support the 100-micron silicone lens, including titanium mesh and fiberglass mesh.

A photo of one of the new titanium mesh lenses is shown in Fig. 2, during an outdoor measurement of the lens optical efficiency. The lens is focusing onto a triple-junction solar cell with a 2 cm x 2 cm active area, as discussed in the Section IV below. The photo-etched titanium mesh is very thin (50 microns), ultra-light (about 0.2 gram for a 10 cm x 10 cm mesh in the photo), and high in open area (96%). It is also equipped with tiny corner holes to facilitate low-stress mounting to a carbon fiber structure (not the black 3D-printed plastic structure for ground testing shown in Fig. 2). In the past year, we have produced prototype lenses of this type with a mass/aperture area of only 0.11 kg/m^2, the lightest lenses we have ever made. For comparison, the lenses some of our team members made for the SCARLET array on Deep Space 1, which flew from 1998-2001, had a mass/aperture area of about 0.6 kg/m^2. Note that the 10 cm x 10 cm lens aperture area divided by the 2 cm x 2 cm cell active area is 25X for this concentrator module. The active area of solar cell surrounding the small focal spot provides ± 2 degree sun-pointing tolerance without significant power loss.

We have developed a simple method of measuring the lens optical efficiency in outdoor testing, based on the method we

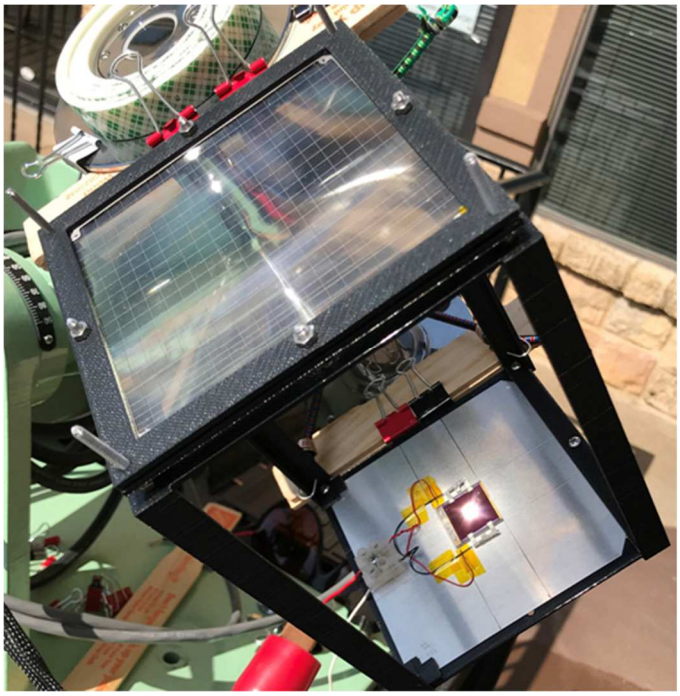

Fig. 2. Outdoor Testing of New Titanium Mesh Lens

and others have used in the past for terrestrial solar concentrators. We first measure the short-circuit current of the cell with the lens in place. We next measure the short-circuit current of the cell with the lens replaced with a black plate with a square aperture hole to allow only direct sunlight to hit the solar cell, while blocking diffuse light, as shown Fig. 3. The sides of the concentrator are also covered with a black material

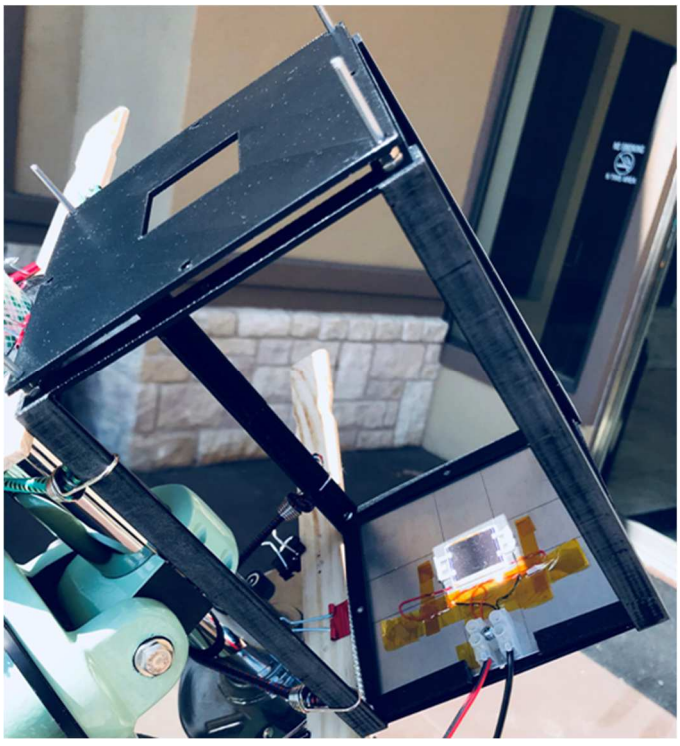

Fig. 3. One-Direct-Sun Outdoor Test.

to block diffuse light from hitting the cell (not shown in Fig. 3). This allows us to measure the short-circuit current for one-direct-sun irradiance. A normal incidence pyrheliometer (NIP) is used to make certain that the direct solar irradiance is the same for both tests (with and without lens).

The short-circuit current gain is the ratio of these two short-circuit current measurements. This gain is compared to the geometric concentration ratio of 25X for the concentrator module to provide the net optical efficiency of the lens. Spectral analysis shows that the top junction of a three-junction cell (or four-junction cell) is the current-limiting junction for both terrestrial sunlight and space sunlight, implying that the outdoor test results will also be applicable to space. Fig. 4 shows typical current-voltage (IV) curve measurements for both tests, with and without the titanium mesh lens in place. For this test, the current gain was 21X and the lens optical efficiency was 84%.

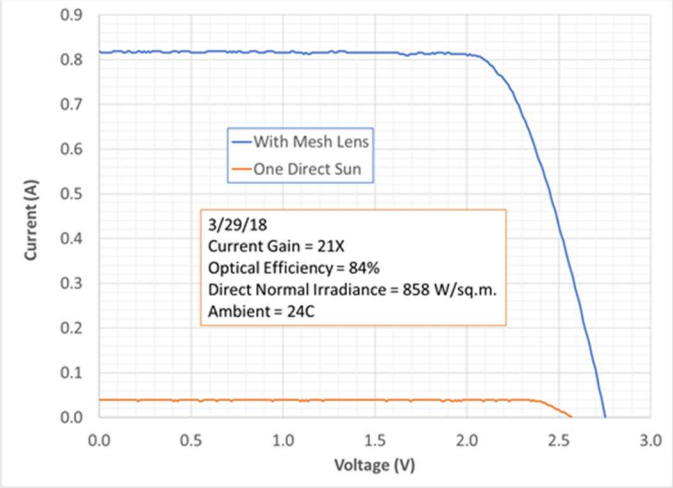

Fig. 4. IV Curve Measurements from Outdoor Test.

We have also recently tested other lens configurations, including pure silicone lenses (for reference) without mesh or superstrates, lenses with silicone prisms molded onto 100-micron CMG glass superstrates, and lenses with embedded fiberglass superstrates, as shown in Fig. 5. While results vary from day to day with the varying sky conditions and solar spectrum, we typically find these results for the different lens constructions:

- Pure Silicone Lenses: About 90% Optical Efficiency.
- Glass Superstrate Lenses: About 90% Optical Efficiency.
- Embedded Mesh Lenses: About 85% Optical Efficiency.

These results are consistent with expectations, since the mesh blocks about 4-5% of the light.

We have also developed practical manufacturing techniques for all styles of point-focus lenses. However, we have encountered some production issues with the glass superstrate lenses and with the embedded metal (titanium or stainless) mesh lenses. When we remove the lens molding tool from the cured and completed lens assembly, we must take care to avoid

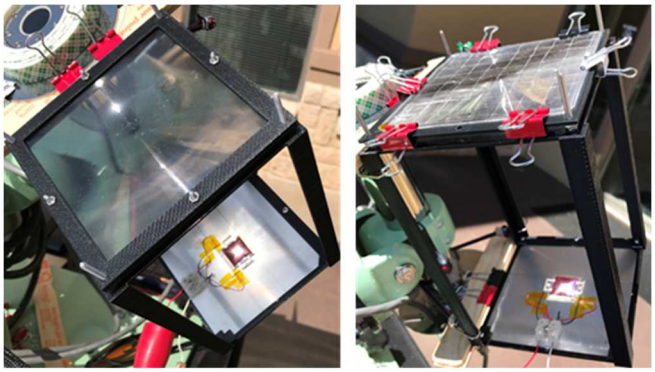

Fig. 5. CMG Glass Superstrate Lens (Left) and Embedded Fiberglass Mesh Lens (Right).

cracks in the thin glass superstrate or to avoid bending or localized distortions in the metal mesh. We have proposed a novel low-cost, high-volume solution to this problem and hope to implement this process for future lens production.

IV. Recent Cell Developments

In the past year, we have done preliminary design and analysis work on an advanced inverted metamorphic multi-junction (IMM) cell, and actual hardware development of a 3-junction germanium-based cell for the 25X concentrator. The IMM cell will need to be mounted to a high-thermal conductivity carrier rather than the traditional ceria-doped glass carrier to tolerate the high peak irradiance produced by the lens. Aluminum nitride is a leading candidate for this IMM cell carrier. For the 3-junction cell, we have also selected aluminum nitride as a heat spreader and dielectric carrier for the germanium-based cell.

For the 3-junction cell, we have developed a novel tapered gridline design to minimize both gridline obscuration loss under the focal spot and also gridline resistance losses in conducting the current from the focal spot to the busbars on both edges of the cell, as shown in Fig. 6. The focal spot is much smaller than the cell active area to accommodate sun-pointing errors. Since sun-pointing errors will be statistically distributed about a mean of approximately zero over the course of a mission, the focal spots on the large number of cells in a sizable space array will

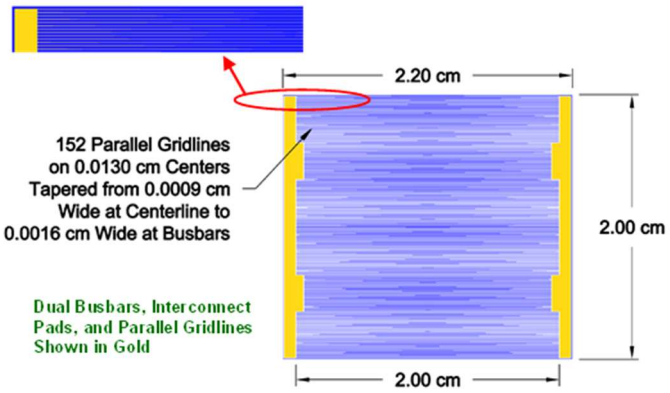

Fig. 6. New 3-Junction Cell Design.

spend more time near the center of the cells than near the edges or corners of the cells. Thus, tapered gridlines should maximize the power output over the mission. The gridline spacing was optimized in the usual fashion by trading off power loss from gridline obscuration with power loss from series resistance.

,The new 3-junction cells (with top tabs attached) have been produced and delivered by SolAero, with one shown in Fig. 7. Based on thermal analysis, we have selected the cell mounting approach shown in Fig. 8. Fig. 9 shows the expected cell temperature distribution for an array to sun distance of 1 AU, with a peak cell temperature of 89°C for a 3-junction cell. The operating cell temperature will be even lower for a future higher efficiency IMM cell.

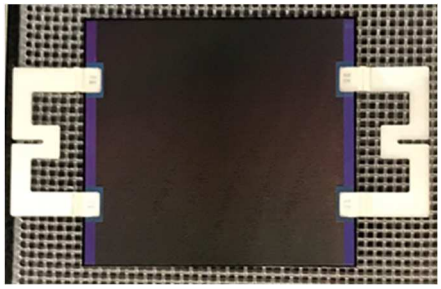

Fig. 7. Photo of 3-Junction Cell with Tabs.

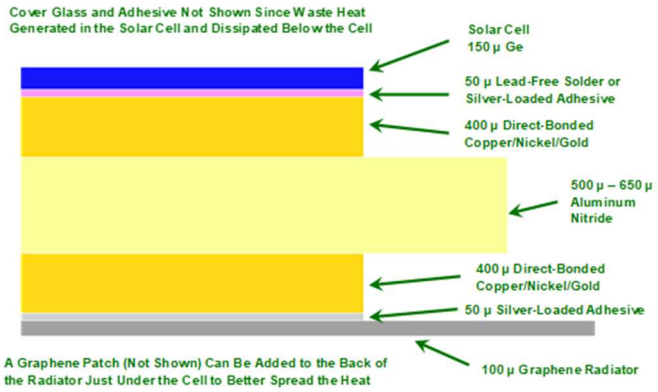

Fig. 8. 3-Junction Cell Mounting Approach.

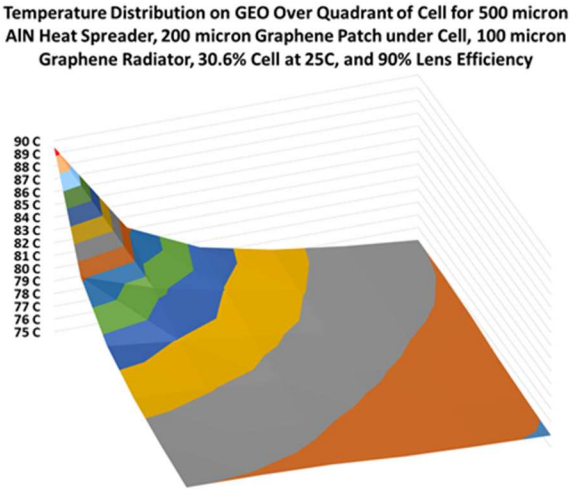

Fig. 9. Cell/Radiator Thermal Analysis Results at 1 AU.

V. Recent Graphene Radiator Developments

Under an ongoing NASA Phase I STTR contract, our research institution partner, the University of Connecticut (UCONN), is developing novel methods of depositing graphene onto aluminum foil to form the bi-material radiator. Water suspensions of graphene (12-15 mg/ml) have been prepared from graphite, and high quality/low defect, 5-6 layer graphene of average lateral flake dimensions of ~1 µm has been confirmed by TEM and Raman spectroscopy. These suspensions were successfully coated onto aluminum foil and the coatings (10 µm) were stable when subjected to multiple thermal cycles (-65 to 100 °C). Future work includes depositing thicker graphene layers (40 µm) onto larger pieces of aluminum foil to form full-size radiators (10 cm x 10 cm).

For the 25X concentrator radiator, we are exploring various graphene layer thicknesses from 40 µm to 100 µm, as well as 200 µm "patches" of graphene under the cell. Since a single monatomic layer of graphene is only 0.35 nm thick, the layers we need are many tens of thousands of overlapping layers of monatomic graphene. These numerous monatomic layers are typically held together with van der Waals forces, which can lead to mechanical failures between layers when a device like a solar cell assembly is adhesively bonded to the outermost layer. We believe we have a solution to this problem with our composite aluminum foil/graphene radiator approach. The solar cell package is bonded to the aluminum foil, where adhesion is not a problem. The graphene is deposited onto the back of the aluminum foil to enhance lateral thermal conduction of waste heat from the cell outward over the full radiator area, since graphene has a much higher thermal conductivity and a much lower density than aluminum.

The UCONN process leads to outstanding adhesion of the deposited graphene to the aluminum foil. The robustness of the bond has been demonstrated not only through thermal cycling tests, but also by repeatedly flexing the composite material many times and inspecting the graphene which remains firmly attached to the aluminum foil, as shown in Fig. 10. Future work will explore scalable mass-production processes, including printing and spraying, to deposit the graphene in an optimal tapered-thickness pattern from a maximum thickness under the center of the cell to a minimum thickness at the edges of the radiator.

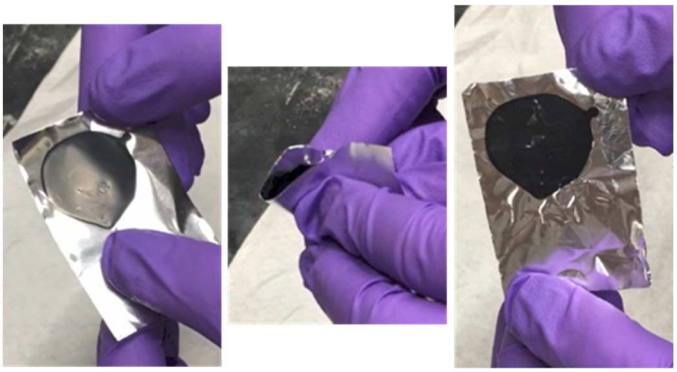

Fig. 10. Flexing Graphene/Aluminum Foil Sample.

VI. 25X Concentrator Module LAPSS Testing

Early in 2018, we tested a 25X concentrator module, including lens, cell assembly, and radiator, for performance under AM0 sunlight at 1 AU irradiance in the SolAero large area pulsed solar simulator (LAPSS) which was used to test line-focus concentrator modules last year, as reported at the last PVSC in Washington, DC. Fig. 11 shows the module under test with the lens in place (top) and with the lens replaced with a diffuse light shield (bottom). Fig. 12 shows the key results of the test.

Note that the lens provided 21.26X short-circuit current (ISC) gain and 22.18X power gain compared to the one-sun values. The ISC Gain divided by the geometric concentration ratio (25X) provides the net optical efficiency of the lens, 85% for the LAPSS test. The lens used in the test module was a pure silicone lens which was previously measured at 90% optical efficiency in outdoor testing. We believe the difference in measurements is due to the much closer light source for the LAPSS test (8 meters versus 1 AU for the sun), and differences

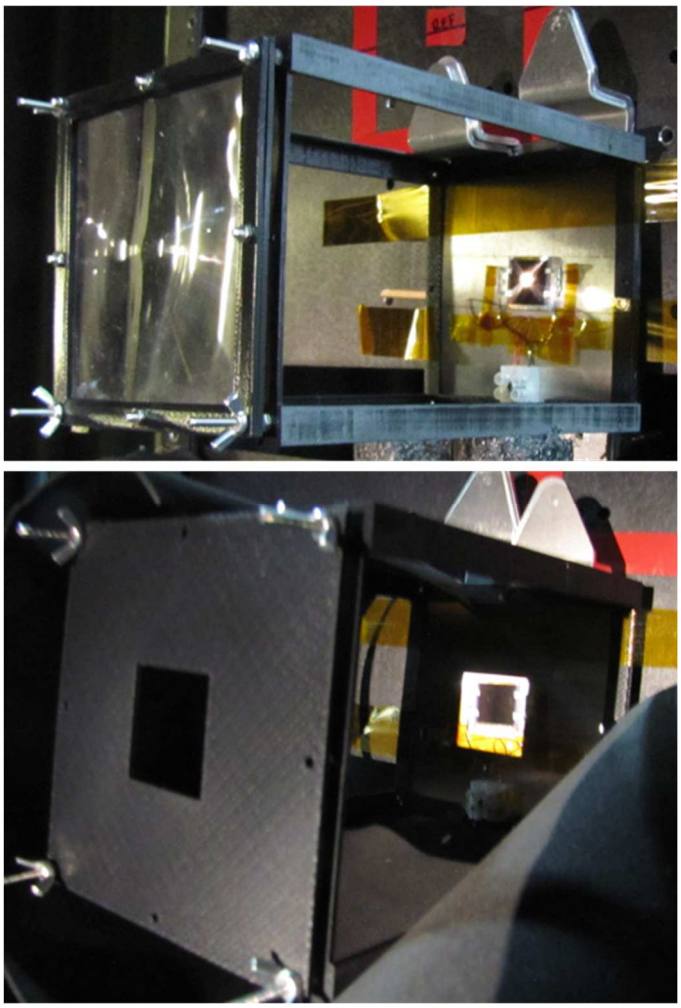

Fig. 11. 25X Concentrator Module in SolAero LAPSS Testing with Lens Irradiance (Top) and One-Sun Irradiance (Bottom).

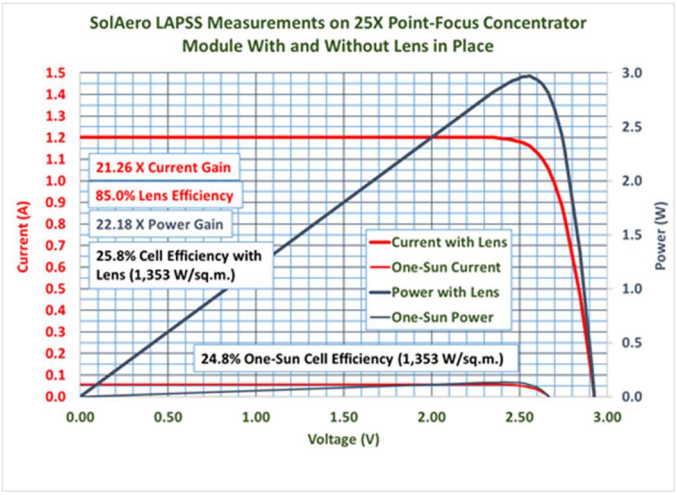

Fig. 12. SolAero LAPSS Test Results.

in the two solar spectra (simulated AM0 in the LAPSS versus approximately AM1.5D in outdoor testing). The cell efficiency (under both one-sun and lens irradiance) was lower than expected based on prior concentrator cell tests. Post-test inspections revealed that the cell gridlines were about 45% wider than specified in Fig. 6 above, due to the very tight program schedule which didn't provide for metallization process optimization. The gridline shadowing loss therefore lowered cell ISC more than expected. But the overall results of the LAPSS test confirmed the expected performance gain (current and power) for the 25X concentrator compared to one-sun results.

VII. Performance Metrics and Cost Savings

As we gather experimental performance data and as we refine our performance and cost models, we are confirming that the new 25X concentrator technology offers exceptional performance metrics and cost savings compared to conventional one-sun solar arrays. For example, the 25X point-focus concentrator saves about 95% of the sophisticated and relatively expensive multi-junction cell area and cost compared to a one-sun array. The mass of cell radiation shielding (front and back) is also reduced by about 95%. These cost and mass savings are particularly important for high-power missions (e.g., solar electric propulsion) and deep space missions (to Jupiter and beyond.

Table I shows the beginning of life (BOL) cell, lens, and concentrator module efficiency estimates for missions to 1 AU and 5 AU, respectively. These estimates are extrapolated from the LAPSS results discussed above to include straightforward improvements in cells and lenses, including:

- Correct the width of gridlines on future cells
- Lower the sheet resistance of emitters on future cells
- Add a refractive prismatic cell cover to the cell
- Improve the lens molding process
- Move from the 3-junction to 4-junction IMM cells

TABLE I
EXTRAPOLATED PERFORMANCE AT 1 AU AND 5 AU

Item	Recent LAPSS Results*	Correct Grid Width*	Reduce Emitter Sheet Resistance*	Add Prismatic Cell Cover*	Improved Lens*	1 AU Future 4J Cell*	Extrapolate to 5 AU***
Cell Efficiency	25.8%	26.6%	27.4%	29.8%	29.8%	35.0%	45.2%
Lens Efficiency (CMG/Silicone Lens)	85.0%	85.0%	85.0%	85.0%	90.0%	90.0%	90.0%
Concentrator Module Efficiency (CMG/Silicone Lens)	21.9%	22.6%	23.3%	25.4%	26.9% **	31.5%	40.6%
Concentrator Module Efficiency (Mesh/Silicone Lens)						29.8%	38.4%
Footnotes:							
*at 25C, 1AU AM0, 1,353 W/sq.m.							
** > 27% Demonstrated in 2014 for Earlier 25X Concentrator							
***at -120C, 5AU AM0, 54 W/sq.m.							

With these improvements, for a concentrator module using a thin CMG glass superstrate, the resultant module efficiency will be over 31% at 1 AU and over 40% at 5 AU. For a concentrator module using an embedded mesh, these efficiency values will be nearly 30% and over 38%, respectively.

NASA is particularly interested in advanced space photovoltaic concentrator technology for future deep space missions to 5 AU and beyond. A major NASA technology development program has been underway for more than two years to develop game-changing solar arrays for such deep space missions. The program is called Extreme Environments Solar Power (EESP). NASA has specified a radiation environment for EESP that is approximately 10X higher than for the solar array on the recent successful JUNO mission to Jupiter [4]. For JUNO, the selected radiation shielding was 14 mils equivalent fused silica on the front of the cell and 30 mils equivalent fused silica on the back of the cell, resulting in an estimated total equivalent 1 MeV electron fluence at the cell of approximately 4 x $10^{14}e^{-}/cm^2$ [4]. For EESP, NASA specified 4 x $10^{15}e^{-}/cm^2$ equivalent 1 MeV electron fluence [5]. Fortunately, JPL, SolAero, and Aerospace Corporation performed tests on both 3-junction and 4-junction cells to these exposure levels [5]. Fig. 13 shows their key results, with the top curve added by our team. The solid gold curve shows results at 5 AU irradiance and -125C cell temperature for a one-sun cell, while the solid green curve shows the same results for the same one-sun cell at 10X the 5 AU irradiance and -125C cell temperature. This test was to show the effect of 10X concentration on the cells. The green curve shows higher efficiency and lower radiation degradation than the gold curve.

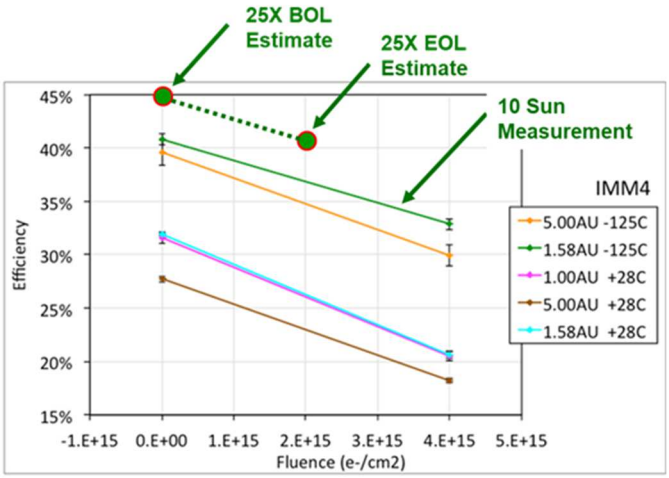

Fig. 13. EESP Radiation Tests of 4-Junction IMM Cells.

Our team has extrapolated these results to our 25X concentrator, as shown by the top dashed-green curve in Fig. 13. By optimizing our small (4 cm^2) cell and operating it at more than twice the 10X concentration, the cell efficiency will be higher than for the large-area one-sun cell under 10X concentration. We estimate the BOL cell efficiency to be 45% (Table I above) rather than the 41% for the one-sun cell at 10 suns, as shown by the data point in Fig. 13. We can also more heavily shield the small cell with a tiny mass penalty due to the 25X concentration. Fortunately, the cell radiation fluence for 30 mils of equivalent fused silica shielding was already calculated for JUNO [4]. By applying the 10X JUNO to EESP radiation exposure factor, we obtain about 2 x $10^{15}e^{-}/cm^2$ equivalent 1 MeV electron fluence for 30 mils of equivalent fused silica shielding front and back. Assuming the same rate of degradation as for the 10-sun measurement, we obtain the end-of-life (EOL) cell efficiency estimate of 41% for the 25X cell, shown by second large data point on the top dashed green curve of Fig. 13. This is equivalent to a cell radiation degradation factor of 90% from EOL to BOL for the EESP mission. Note also that the EOL cell efficiency for the one-sun cell (solid gold curve) is 30% compared to the 41% for the 25X cell. This huge advantage will also be achieved with much lower mass for cell shielding, since 30 mils of shielding for the small 25X cell is equivalent in mass to only 1.2 mil of shielding for the one-sun cell.

We have also tested lens samples comprising silicone with embedded mesh to more than 10X the JUNO low-energy proton radiation exposure test level for optical components [4] with negligible optical and mechanical degradation. Finally, the estimated concentrator module specific power at 1 AU and 25C is over 800 W/kg at BOL, and the estimated cost per Watt is less than half the cost for a one-sun cell.

VIII. REFERENCES

[1] M. O'Neill, A. McDanal, H. Brandhorst, K. Schmid, P. LaCorte, M. Piszczor, M. Myers, "Recent space PV concentrator advances: more robust, lighter, and easier to track," *42nd IEEE Photovolt. Specialist Conf.*, 2015.

[2] M. O'Neill, A. McDanal, H. Brandhorst, B. Spence, S. Iqbal, P. Sharps, C. McPheeters, J. Steinfeldt, M. Piszczor, M. Myers, "Space photovoltaic concentrator using robust Fresnel lenses, 4-junction cells, graphene radiators, and articulating receivers," *43rd IEEE Photovolt. Specialist Conf.*, 2016.

[3] M. O'Neill A. McDanal, M. Piszczor, M. Myers, P. Sharps, C. McPheeters, J. Steinfeldt, "Line-focus and point-focus space photovoltaic concentrators using robust Fresnel lenses, 4-junction cells, & graphene radiators," *44th IEEE Photovolt. Specialist Conf.*, 2017.

[4] S. Dawson, P. Stella, W. McAlpine, B. Smith, "JUNO photovoltaic power at Jupiter," *10th International Energy Conversion Engineering. Conference*, 2012.

[5] A. Boca, P. Stella, C. Kerestes, P. Sharps, "Solar arrays for low-irradiance low-temperature and high-radiation environments," NASA EESP Base Period Final Report, JPL, April 26th, 2017.